Stability of Viscous Fingering in Uniport Lifted Hele Shaw Cell

Sachin D. Kanhurkar*, Prasanna S. Gandhi*, Amitabh Bhattacharya†

***Department of Mechanical Engineering, Indian Institute of Technology, Bombay**

†Department of Applied Mechanics, Indian Institute of Technology, Delhi

Abstract

Lifted Hele Shaw cells typically display viscous fingering of liquids, which in turn leads to branched fractal patterns in the absence of any anisotropies. Recently, experiments involving parallely lifted Hele Shaw cells with holes in the cell plates, also termed as "multi-port lifted Hele Shaw cells (MLHSCs)", have been used to generate more regular mesh-like patterns in the liquid film. Although such patterns promise usefulness in several applications, their spatio-temporal evolution needs to be theoretically and numerically understood for better synthesis. We are able to understand how the interface stability depends on Capillary number and film thickness. We attribute this dependence of hole shape on flow parameters to the pressure gradient field present within the fluid.

Introduction

Fundamental process: Squeezing of viscous liquid followed by separation

- While separating the two plates causes the surrounding low-viscosity fluid (e.g. air) pushed the high viscosity fluid, in turn leading to viscous fingering, caused primarily by Saffman-Taylor instability of the interface.
- Holes in the upper plate create localized high pressure regions within the liquid film and thus acts as source for the air to penetrate into the liquid film while the lifting is in progress.

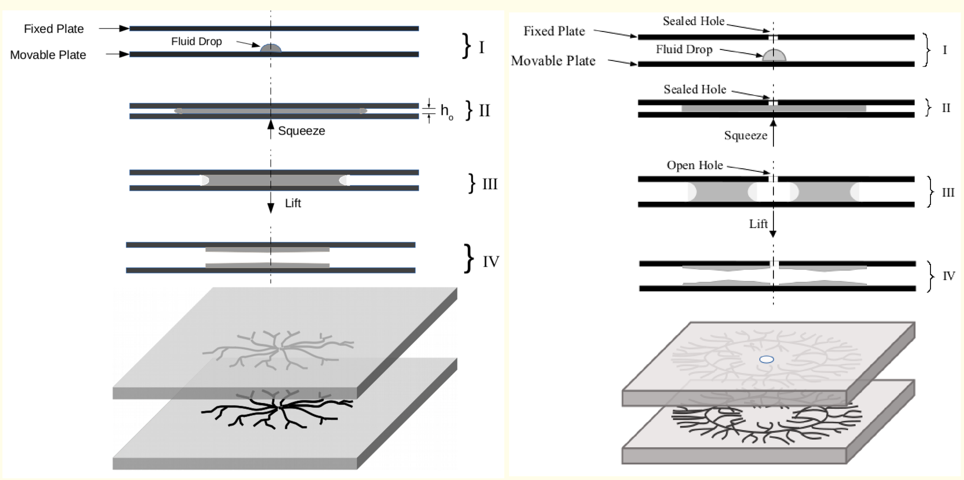

(a) (b)

Figure 1: Schematic of different stages of Lifted Hele-Shaw Cell (LHSC) experiments (a) without and (b) with hole in the top plate [Ref. Bhattacharya et al., 2019].

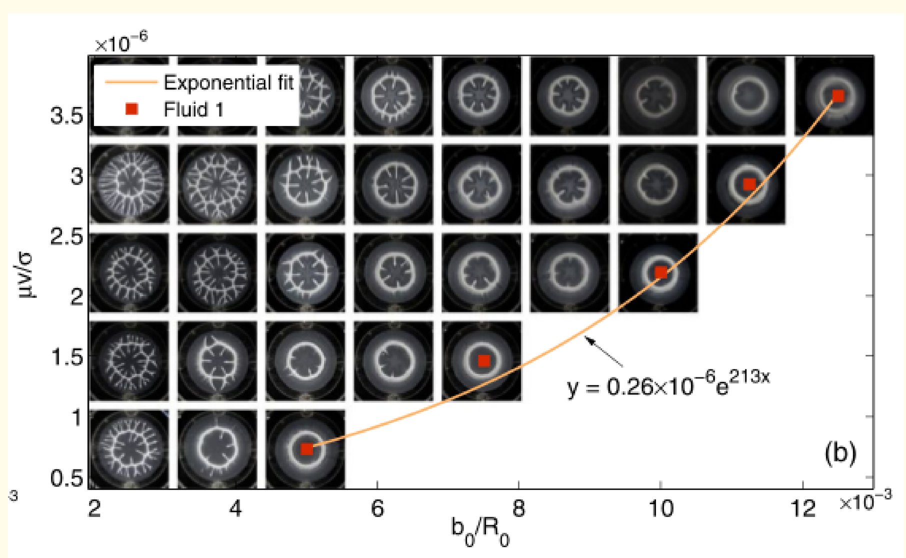

Figure 2: Final top view of liquid film formed on a plate for different values of Ca and h_0/R_0 [Ref. ul Islam, T. and Gandhi, P. S. (2017)].

- Inner and outer interface are more stable for low Capillary number and high dimensionless film thickness.

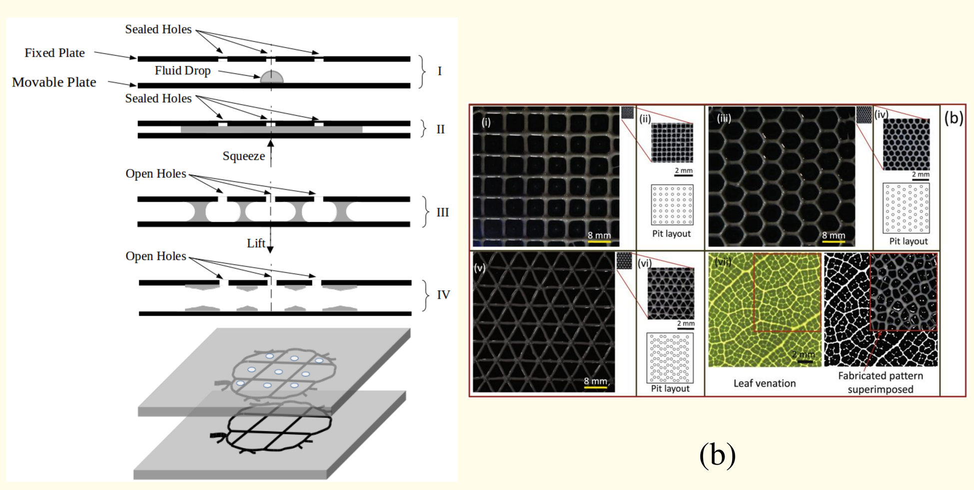

(b)

(a)

Figure 3: (a)Schematic of different stages of MLHSC experiments. (b) Different meshes developed using MLHSC, Top Left: Square mesh, Top Right: Hexagonal mesh, Bottom Left: Triangular mesh, Bottom Right: Pattern developed to match a mesh pattern on a leaf [ul Islam, T. and Gandhi, P. S. (2017)].

Motivation and Objectives

1. Selection of parameters to get different mesh and fractal pattern in lifted Hele Shaw cell
2. Understand phenomenon without expensive experiments
3. Understand the dependency of shape formation on the different parameters

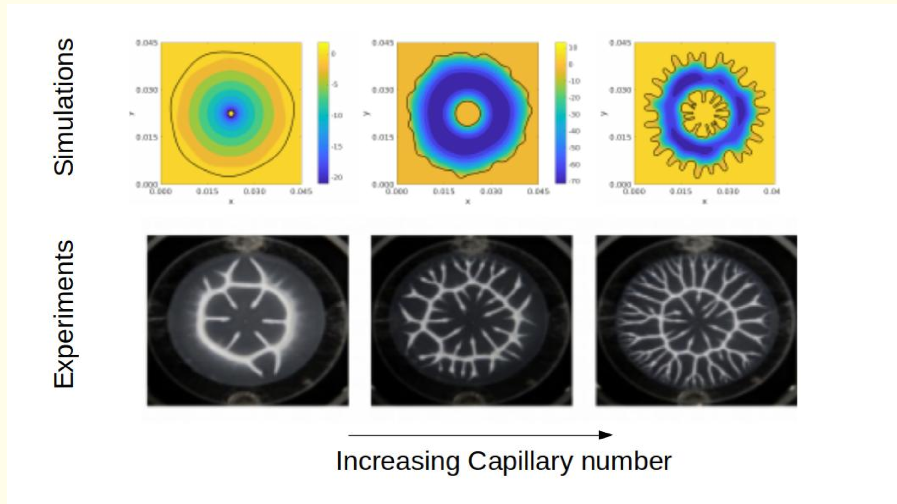

Figure 4: LHSC with a hole [Ref. Bhattacharya et al., 2019].

Governing Equations

- The equations which govern the system are: Pressure Poisson Eqn. $\nabla^2 p = \frac{12\mu}{h^3}\frac{dh}{dt}$,
- Young-Laplace boundary condition: $p(R_\alpha, \theta, t) = \sigma \cdot \kappa_\alpha(\theta, t)$, where $\kappa_\alpha(\theta, t) = -\mathbf{n} \cdot \frac{d\mathbf{t}}{ds}$ is curvature of the interface $\mathcal{C}_\alpha$, $\alpha \in \{out, in\}$ at azimuthal location θ and time t, while s is the distance along the curve.
- Kinematic boundary condition : $\frac{\partial R_\alpha}{\partial t} = \left(u_r - \frac{u_\theta}{r}\frac{\partial R_\alpha}{\partial \theta}\right)\Big|_{r=R_\alpha}$.

Nondimensional parameters governs the dynamics of system:

- Capillary number: $\mathrm{Ca} = \frac{\mu}{\sigma}\frac{dh}{dt}$ ratio of the viscous to surface tension force,
- Nondimensional height: $h^* = \frac{h_0}{R^0_{out}(0)}$ characterizes liquid film thickness,
- Radius ratio: $\gamma = \frac{R^0_{out}(0)}{R^0_{in}(0)}$ characterizes initial radial thickness,
- Nondimensional array spacing : $\lambda = \frac{L}{R^0_{in}(0)}$ characterizes the array spacing,
- Nondimensional time : $t^* = t \cdot \frac{dh/dt}{h_0}$ describes time of separation of the plates.

Numerical methodology

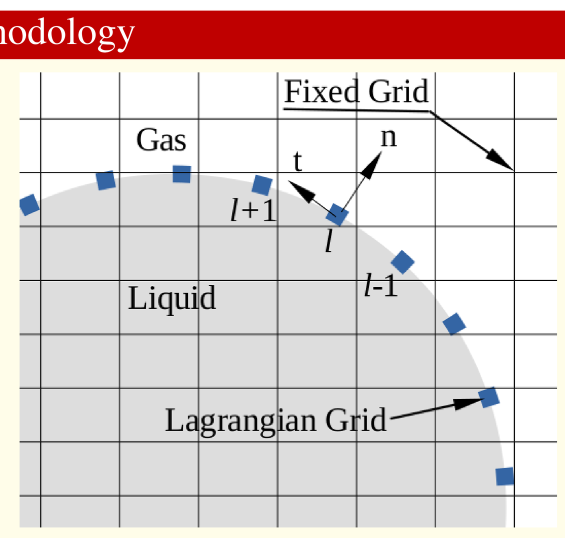

Figure 5: Schematic showing fixed Cartesian grid for representing pressure (black lines) and Lagrangian nodes (▢) to discretely represent the liquid-gas interface shape. The unit tangent ($\mathbf{t}$) and normal ($\mathbf{n}$) vector has also been shown at an interface node here. The shaded region represents the liquid film.

- Front tracking method to evolve the interface in time and space.
- At each time step, we first use a sharp interface method to solve the Poisson equation with the Young-Laplace boundary condition to obtain p at the grid points inside the liquid. We then use kinematic boundary condition to evolve interface position $\mathbf{X}^\alpha$.

Results

LHSC with a single hole

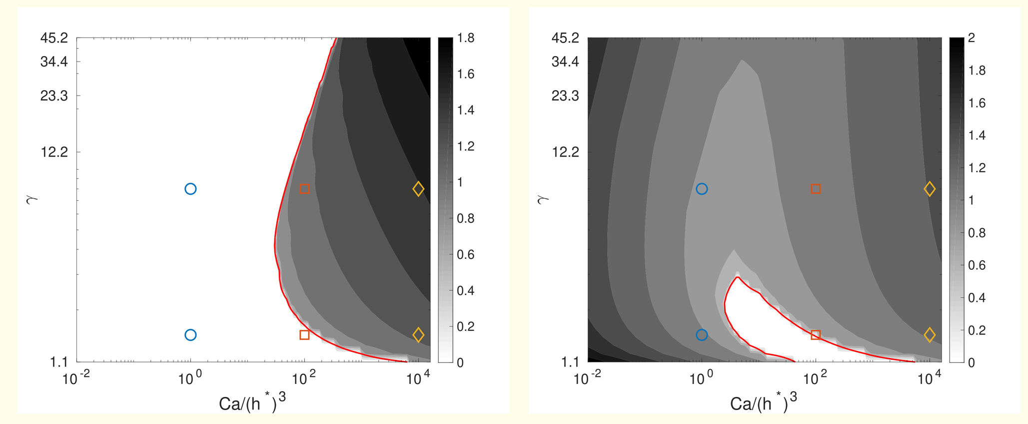

(a) Inner interface (b)Outer interface

Figure 6: Phase map from linear stability analysis (LSA) showing the stability regime for LHSC with hole for Fig. a: inner and Fig. b: outer interface over the γ and $\mathrm{Ca}/(h^*)^3$ [Ref. Bhattacharya et al., 2019].

- For high $\mathrm{Ca}/(h^*)^3$, both the inner and outer interfaces contain a larger band of wavenumbers with high growth rate.
- At values of $\gamma \to 1^+$ (i.e. small annular thickness), the interfaces are stable over a much larger range in $\mathrm{Ca}/(h^*)^3$.
- In the presence of a hole, the outer interface is unstable for $\mathrm{Ca}/(h^*)^3 \ll 1$ for perturbations with small wavenumber.

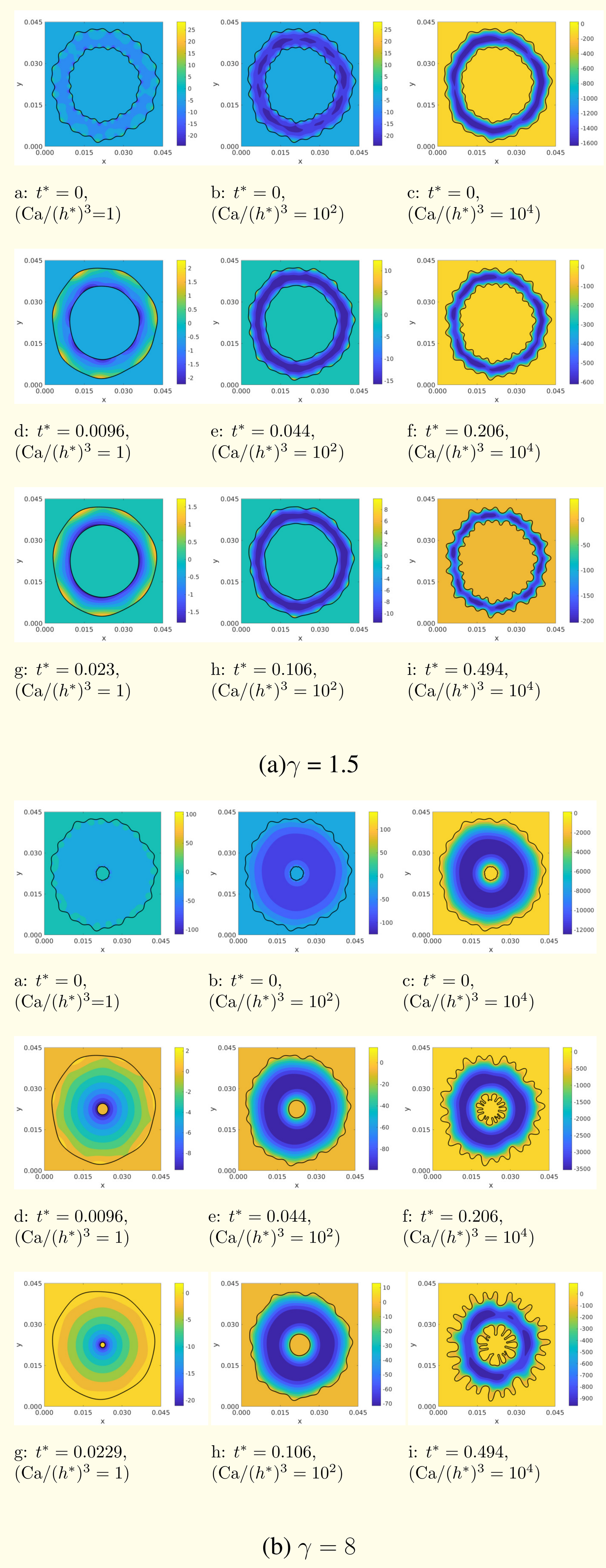

Figure 7: Pattern formed on plate in LHSC with the hole for $\gamma = 1.5$ and $\gamma = 8.0$, contour shows the pressure distribution, [Ref. Bhattacharya et al., 2019].

Possible Impact

Enables fast and cost effective biomimicking resulting in several applications

1. Biological Application : drug screening platform for multiple drugs, mimicking of biological systems - like renal , lung system, leaf venation, nature inspired lab on chip, organ-on chip(ex. Blood brain barrier on chip)
2. Engineering Application : Efficient chip cooling, solar cell electrodes, capillary pump (for point-of-care diagnostics)

Publications

1. Sachin D. Kanhurkar, Vardhan Patankar, Tanveer ul Islam, Prasanna S. Gandhi, and Amitabh Bhattacharya. Stability of viscous fingering in lifted hele-shaw cells with a hole. Phys. Rev. Fluids, 4:094003, Sep 2019.
2. Tanveer ul Islam and Prasanna S Gandhi. Viscous fingering in multiport hele shaw cell for controlled shaping of fluids. Scientific reports, 7(1):16602, 2017.
3. Tanveer Ul Islam and Prasanna S Gandhi. Fabrication of multscale fractal-like structures by controlling fluid interface instability. Scientific reports, 6:37187, 2016.

Acknowledgements

This work was carried out under joint funding from the Ministry of Human Resource Development (MHRD) and Department of Science and Technology (DST) through IMPRINT1 program under Grant No. DSTIMC002.